Hybrid-Mode Computation of Propagation and Attenuation Characteristics of Parallel Coupled Microstrips with Finite Metallization Thickness

Jen-Tsai Kuo, *Member, IEEE,* and Tatsuo Itoh, *Fellow, IEEE*

***Abstract*— The hybrid-mode mixed spectral domain approach (MSDA) is formulated to investigate the dispersion nature of multiple coupled microstrip lines with arbitrary metallization thickness. Incorporated into the solution procedure, a new set of basis functions with $\delta^{-1/3}$ field singularity near conductor edges is found to be effective in calculating both the phase and attenuation constants. The computation of conductor loss is based on the perturbation procedure. Over a broad band of frequency spectrum, excellent agreement is obtained between the calculated results and existing experiment data for the metallic losses of a single microstrip and effective dielectric constants of coupled lines. The influence of finite metallization thickness on the frequency dependent modal propagation and attenuation characteristics is presented for both a three-line and four-line structure.**

***Index Terms*— Attenuation, metallization, microstrip, spectral domain analysis.**

I. Introduction

FINITE metallization thickness is one of the paramount factors that affects the propagation and attenuation characteristics of planar waveguides, especially in high density miniaturized monolithic microwave integrated circuits (MMIC's) used in moderate power purpose or in higher microwave and millimeter-wave frequency bands. As a result of improvements in fabricating high performance complex components in these bands, the design of MMIC's requires simulation tools with more accuracy for finite thickness planar transmission lines [1].

Full-wave analysis of finite thickness planar waveguides has been carried out by several techniques. The mode-matching method (MMM) is a very versatile technique for this purpose [1]–[4]. In [2], for the first time an analysis of finite thickness coplanar strips (CPS's) is performed. The characteristic impedances of CPS's are found to have strong dependence on the strip thickness. By treating the imperfect metallic layers in the same way as the remaining subregions in the waveguide, a two-step mode-matching formulation can handle the calculations of phase and attenuation constants [3], [4]. The finite element method (FEM) is a flexible technique for studying open microstrips [5] and shielded lines with arbitrary metallization cross section [6]. When highly accurate results are pursued, however, these two methods are known to require large computer memory and matrix size even if the cross-sectional metallization contour is of a simple shape. In addition to MMM and FEM, method of lines (MoL) is also found to be well suited to analyze planar waveguides with finite metallization thickness [7].

The spectral domain approach (SDA) [8] is a well-known technique for computing circuit parameters of planar transmission lines for the ease of its formulation and numerical efficiency. The immittance concept [9] further enhances the preprocessing and computing works for multilayer multiconductor structures. Unfortunately, the applicability of the SDA had been limited to infinitely thin lines until the works in [10]–[12] were published. The extended spectral domain approach (ESDA) is employed to analyze lossy coplanar-type waveguides in [10] and single and coupled strip lines in [11]. Coupled integral equations, with spectral dyadic Green's functions and unknown aperture fields as the integrands, are obtained to set up the determinantal matrix equation. A set of basis functions with $\delta^{-1/3}$ field variations is adopted for expanding the unknown aperture fields. This is important since 1) it correctly describes the asymptotic field variation near conductor edges, and 2) the calculation of conductor loss based on the perturbation scheme cannot converge if a $\delta^{-1/2}$ field variation near conductor edge is used [10].

Also of interest is the presentation in [12]. A two-level model is used to approximate each moderately thick conductor in a layered dielectric media. In this model, the vertical walls of the conductors are neglected and removed. The layered region between the top and bottom surfaces of the center conductors is then entirely filled with air so that the spectral Green's functions can be easily obtained. The use of this model, however, is limited by the metallization thickness to strip width and to strip spacing ratios [12].

In this paper, we employ the mixed spectral domain approach (MSDA) [13] to investigate the dispersive propagation characteristics of parallel coupled microstrips with rectangular line cross sections. In the MSDA formulation, simultaneous linear algebraic equations, in contrast to the coupled integral equations in the ESDA, are obtained for determining the phase constants. As will be seen later, this method can be applied to multimicrostrip structures with arbitrary metal-

Manuscript received May 3, 1996; revised October 18, 1996. This work was supported by the National Science Council, Taiwan, under Grants NSC 86-2213-E-009-068

J.-T. Kuo is with the Department of Communication Engineering, National Chiao Tung University, Hsinchu 300, Taiwan, R.O.C.

T. Itoh is with the Electrical Engineering Department, University of California at Los Angeles, Los Angles, CA 90024 USA.

Publisher Item Identifier S 0018-9480(97)00835-1.

lization thickness to strip width and to strip spacing ratios, since the electromagnetic boundary conditions along the entire perimeter of each conductor are fully satisfied. A set of basis functions with $\delta^{-1/3}$ field behavior, other than that in [10], is incorporated into the solution procedure. It is found that, for expanding electrical fields in apertures of more than ten times the strip width, only four basis functions are enough for accurately calculating the modal parameters. It results in a determinantal matrix of relatively small size.

This paper is motivated by the following two facts. The first is that the dispersive nature of finite thickness multimicrostrip structures has been studied by only a limited number of literatures [2]. The second is that, although the metallization thickness plays a minor role in a single microstrip [3], its influence on the propagation and attenuation characteristics of coupled microstrips still needs investigating.

The presentation is organized as follows. Section II briefly formulates the MSDA and lists the employed set of basis functions. In Section III, the validity of the calculated results is checked against existing measurement data. The influences of finite metallization thickness and interline spacing on the propagation and attenuation characteristics of two multimicrostrip structures are then presented and discussed. Section IV draws the conclusion of this presentation.

II. Formulation

A. The Determinantal Equation

The cross-section view of the shielded parallel coupled N-line microstrip structure under investigation is shown in Fig. 1(a). The black boxes sitting on the substrate are signal strips with thickness t. According to the equivalent principle illustrated in [13], the waveguide can be analyzed by its equivalent structure consisting of $N+3$ (0 through $N+2$) rectangular cells as in Fig. 1(b). At $z=h_1$ and $z=h_1+t$, each aperture surface can be short-circuited and restored by a magnetic current source $\boldsymbol{M}$

$$\boldsymbol{M}=\boldsymbol{n}\times\boldsymbol{E} \tag{1}$$

where $\boldsymbol{E}$ is the original tangential electrical field column vector $[E_x, E_y]^{\mathrm{T}}$ before it is short-circuited and $\boldsymbol{n}$ is the outward normal vector of the surface. On both sides of each aperture, the equivalent $\boldsymbol{M}$ sources have identical magnitude but opposite signs, since the tangential $\boldsymbol{E}$ fields must be continuous.

Since each rectangular cell has perfectly conducting sidewalls, the electromagnetic fields inside the cell can be expressed by the Fourier series. It means that the SDA [8] can be invoked to calculate the fields if the $\boldsymbol{M}$ sources are known. In cell k, $1\le k\le N+1$, after all the field components are transformed into the spectral domain with respect to

$$a_{kn}=n\pi/S_k, \qquad n=0,2,\cdots \tag{2}$$

one can find that the aperture tangential magnetic fields $\tilde{\boldsymbol{H}}$ at $z=(h_1+t)^-$ and the equivalent magnetic current sources

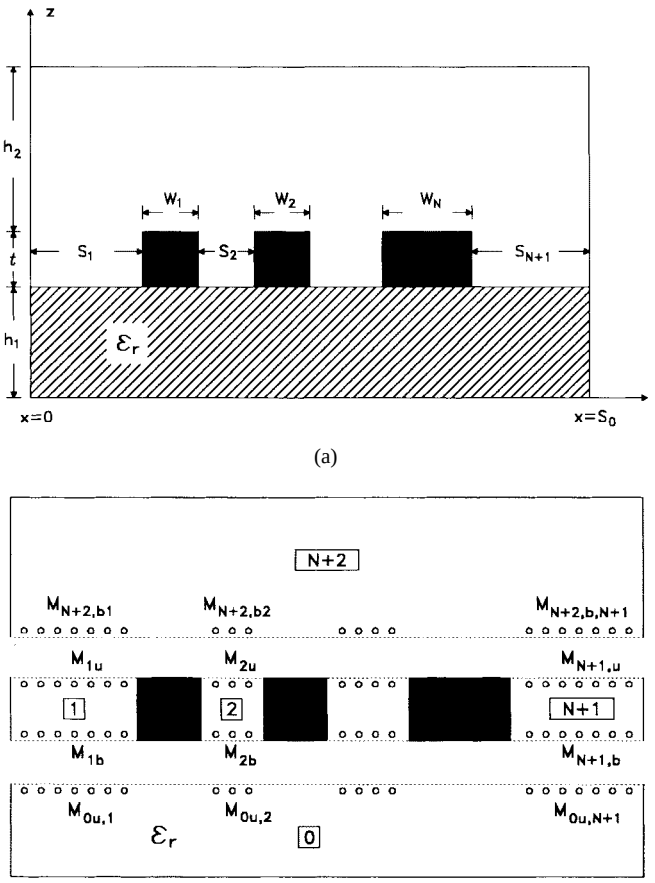

Fig. 1. Parallel coupled N-line microstrip structure with finite metallization thickness. (a) Structure. (b) Equivalent structure for calculating field solutions with equivalent magnetic currents at short-circuited aperatures.

$\tilde{\boldsymbol{M}}$ are related by

$$\begin{bmatrix}\tilde{H}_x\\ \tilde{H}_y\end{bmatrix}_{ku}=\begin{bmatrix}\tilde{G}^{uu}_{xx} & \tilde{G}^{uu}_{xy}\\ \tilde{G}^{uu}_{yx} & \tilde{G}^{uu}_{yy}\end{bmatrix}_k\begin{bmatrix}\tilde{M}_x\\ \tilde{M}_y\end{bmatrix}_{ku}+\begin{bmatrix}\tilde{G}^{ub}_{xx} & \tilde{G}^{ub}_{xy}\\ \tilde{G}^{ub}_{yx} & \tilde{G}^{ub}_{yy}\end{bmatrix}_k\begin{bmatrix}\tilde{M}_x\\ \tilde{M}_y\end{bmatrix}_{kb} \tag{3}$$

where u and b represent the field quantities at $z=(h_1+t)^-$ and $z=h_1^+$, respectively, the overhead tilde denotes the corresponding field variable or function in the transform domain, and the $\tilde{G}$'s are the spectral dyadic Green's functions. The relation between the magnetic fields at $z=h_1^+$ and the $\tilde{\boldsymbol{M}}$ sources can be obtained in a similar fashion. For cells 0 and $N+2$

$$\begin{bmatrix}\tilde{H}_x\\ \tilde{H}_y\end{bmatrix}_{0u}=\begin{bmatrix}\tilde{G}^{uu}_{xx} & \tilde{G}^{uu}_{xy}\\ \tilde{G}^{uu}_{yx} & \tilde{G}^{uu}_{yy}\end{bmatrix}_0\cdot\sum_{i=1}^{N+1}\tilde{\boldsymbol{M}}_{0u,i} \tag{4a}$$

and

$$\begin{bmatrix}\tilde{H}_x\\ \tilde{H}_y\end{bmatrix}_{N+2,b}=\begin{bmatrix}\tilde{G}^{bb}_{xx} & \tilde{G}^{bb}_{xy}\\ \tilde{G}^{bb}_{yx} & \tilde{G}^{bb}_{yy}\end{bmatrix}_{N+2}\cdot\sum_{i=1}^{N+1}\tilde{\boldsymbol{M}}_{N+2,b,i}. \tag{4b}$$

Note that if the conducting wall at $x=S_0$ is of magnetic type, the values of α_{0n}, $\alpha_{N+1,n}$, and $\alpha_{N+2,n}$ must be changed accordingly.

To solve the unknown aperture fields, one can follow the Galerkin procedure [13] to set up the determinantal matrix

equation. First, the $\boldsymbol{M}$ sources are expanded by a suitable set of known basis functions which will be discussed later. Then the testing procedure is given in the spatial domain. By utilizing the Parseval's theorem, one can obtain $2N+2$ sets of simultaneous linear algebraic equations for solving the phase constants and the unknown equivalent $\boldsymbol{M}$ sources in the $2N+2$ aperture surfaces. If N_b basis functions are used for both M_x and M_y in each aperture, the size of the final matrix is only $4(N+1)N_b$.

B. The Set of Basis Functions

In the Galerkin procedure, the equivalent magnetic current sources in apertures of cell k are expanded as

$$M_{xk}^{v}(x) = \sum_{j=1}^{N_b} C_{kj}^{v} M_{xkj}(x) \tag{5a}$$

$$M_{yk}^{v}(x) = \sum_{j=1}^{N_b} D_{kj}^{v} M_{ykj}(x) \tag{5b}$$

where the superscript v stands for u or b and C_{kj}^{v} and D_{kj}^{v} are constants to be solved. To obtain the explicit form of M_{xkj} and M_{ykj}, the behavior of the aperture electric fields should be examined first. At both ends of each aperture S_k, $2 \le k \le N$, in Fig. 1(a), there are 90° conductor corners. Based on the derivation in [14], a set of basis functions can be obtained by expanding the M_x and M_y. We choose

$$M_{xki}^{\pm}(u_k) = (1 \pm u_k)^{2i/3} - 2^{1/3}(1 \pm u_k)^{2(i+1)/3} + 2^{-4/3}(1 \pm u_k)^{2(i+2)/3} \tag{6a}$$

$$M_{yki}^{\pm}(u_k) = (1 \pm u_k)^{2i/3-1} - 2^{1/3}(1 \pm u_k)^{2(i+1)/3-1} + 2^{-4/3}(1 \pm u_k)^{2(i+2)/3-1} \tag{6b}$$

where $u_k = (x - x_{ck})/(S_k/2)$, $-1 \le u_k \le 1$, with x_{ck} being the midpoint of the aperture of cell k, $M_{xkj} = M_{xki}^{+} - M_{xki}^{-}$ and $M_{ykj} = M_{yki}^{+} + M_{yki}^{-}$ for $j =$ odd and $i = (j+1)/2$, and $M_{xkj} = M_{xki}^{+} + M_{xki}^{-}$ and $M_{ykj} = M_{yki}^{+} - M_{yki}^{-}$ for $j =$ even and $i = j/2$. In this way, both M_{xkj} and M_{ykj} are alternated odd and even functions with respect to x_{ck}; when M_{xkj} is even, M_{ykj} is odd and vice versa. Note that the $\delta^{-1/3}$ and $\delta^{2/3}$ field variations near each conducting edge have been incorporated into M_{yk1} and M_{xk1}, respectively. Due to the existence of electrical walls at $x = 0$, only even M_{y1j} and odd M_{x1j} functions are useful for apertures S_1. The same idea is applied to aperture S_{N+1}.

The Fourier transform of $(1+u_k)^{\tau}$ can be derived as closed-form expressions for both small and large $\alpha_{kn}S_k$ products. When $x_{ck} = 0$, it is found that: 1) the transform of $(1-u_k)^{\tau}$ is the complex conjugate of that of $(1+u_k)^{\tau}$; and 2) no matter how many basis functions are used for both M_x and M_y, only the transforms of $(1+u_k)^{-1/3}$, $(1+u_k)^{0}$, and $(1+u_k)^{1/3}$ need deriving, since all terms with higher τ values can be calculated via the following simple recursive formula:

$$\mathbf{F}[(1+u_k)^{\tau}] = \{2^{\tau-1}S_k \exp(j\xi_{kn}) - \tau \mathbf{F}[(1+u_k)^{\tau-1}]\}/j\xi_{kn} \tag{7}$$

where $\xi_{kn} = \alpha_{kn}S_k/2$ and $\tau = m/3$ for $m = 2, 3\cdots$. Thus, the Fourier transforms of the whole set of basis functions can be calculated very quickly.

TABLE I
CONVERGENCE ANALYSIS OF THE MSDA FOR THE FIRST MODAL PHASE AND ATTENUATION CONSTANTS OF A FOUR-LINE MICROSTRIP STRUCTURE AT 20 GHz. $\epsilon_r = 12.9$, $W_1 = W_2 = W_3 = W_4 = h_1 = 0.254$ mm, $S_2 = S_3 = S_4 = 0.0381$ mm, $S_1 = S_5 = 2.54$ mm, $t = 0.03$ mm, $h_2 = 5$ mm

Normalized Phase Constants β/k_o

N_b \ N_s	10^2	2×10^2	5×10^2	10^3	2×10^3	5×10^3	5×10^4
2	3.3666	3.3676	3.3681	3.3681	3.3681	3.3681	3.3681
3	3.2452	3.2482	3.2495	3.2498	3.2499	3.2500	3.2500
4	3.2380	3.2408	3.2438	3.2443	3.2445	3.2446	3.2446
5	3.2371	3.2402	3.2433	3.2439	3.2441	3.2442	3.2442
6	3.2363	3.2398	3.2428	3.2436	3.2438	3.2440	3.2440

Attenuation Constants α (dB/m)

N_b \ N_s	5×10^2	10^3	2×10^3	5×10^3	10^4	2×10^4	5×10^4
2	15.5	15.7	16.0	16.3	16.5	16.6	16.6
3	13.8	14.0	14.2	14.5	14.6	14.6	14.7
4	13.7	13.8	14.0	14.2	14.3	14.4	14.4
5	13.6	13.8	13.9	14.1	14.2	14.2	14.2
6	13.6	13.7	13.8	14.0	14.1	14.2	14.2

C. The Attenuation Constants

After the aperture $\boldsymbol{M}$ sources or the tangential electric fields are obtained, the tangential $\boldsymbol{H}_t$ fields at the conductor surfaces can be calculated. For each mode, the attenuation constant is given by

$$\alpha = P_C/2P_T \tag{8}$$

where P_T is the time-average cross-sectional power flow and P_C is the power consumed by the imperfect conductors, based on the perturbation scheme

$$P_c = \frac{1}{2}R_s \int_S |H_t|^2 \, dl \tag{9}$$

where R_s is the surface resistance of imperfect metal and H_t is calculated from the loss free structure. The integration contour includes the full perimeter of each signal strip and the inner surface of the waveguide housing.

III. RESULTS

In this section, we begin with investigating the convergence behavior of the MSDA for analyzing closely packed thick parallel-coupled microstrips. Then the phase constants for a pair of coupled microstrips and the metallic loss of a single microstrip are checked against existing measured results up to millimeter-wave frequencies. The dependence of the dispersive propagation and attenuation characteristics on the line spacing the metallization thickness are presented and discussed for two multimicrostrip waveguides.

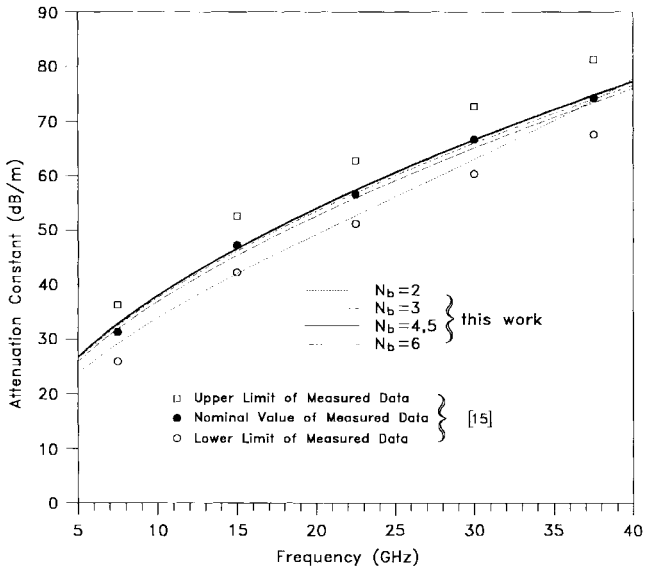

Fig. 2. Comparison of calculated and measured attenuation constants for a single microstrip. $\epsilon_r = 12.9$, $W = 70\ \mu$m, $t = 3\ \mu$m, $h_1 = 100\,\mu$m, $h_2 = 10$ mm, $S_1 = S_2 = 6$ mm, $R_s = 4.1 \times 10^7$ **S**/m.

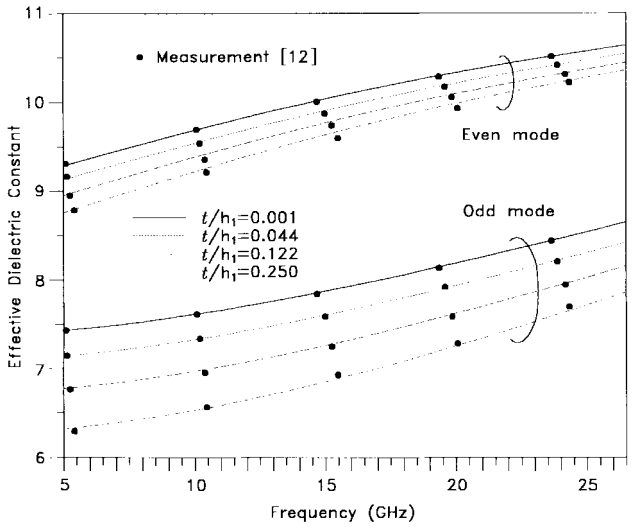

Fig. 3. Comparison of calculated and measured effective dielectric constants for coupled microstrip lines. $\epsilon_r = 12.5$, $W/h_1 = S_2/h_1 = 1$, $h_1 = 0.6$ mm, $h_2 = 10$ mm, $S_1 = S_3 = 6$ mm.

A. Convergence Study and Confidence Check

The convergence behavior of the MSDA technique is examined using a microstrip structure with four equally spaced equal width lines at 20 GHz. In the calculation, the aperture widths $S_1 = S_5 = 10W$, W being the line width, and $h_2 \simeq 20/h_1$ are used to simulate the lines in an open environment, and $S_2 = S_3 = S_4 = 0.15W$ and $t/S_2 \simeq 0.8$ to simulate a crucial situation for the program to obtain converged line parameters. It is because: a) a large number of basis functions N_b for M_x and M_y in the largest apertures can be required since the effective aperture dimensions are 20 times (due to the symmetry about the sidewalls at $x = 0$ and $x = S_0$) the strip width; and b) a large number of spectral summation terms N_s may be required to correctly reflect the field distributions in apertures due to the small ratio $S_2/S_0 \simeq 0.006$.

Table I shows the convergence pattern of the normalized phase constants β/k_o and the attenuation constants α for the first dominant mode of the structure. In the analysis, N_b runs from 2 through 6 and N_s, which is finite for calculation purposes, starts at 10^2 and terminates at 5×10^4. For $N_b = 3$ through 6, the β/k_o values obtained by using $N_s = 10^2$ deviate relatively from those using $N_s = 5 \times 10^4$ by less than 0.25%. The results obtained by $N_s \geq 2 \times 10^3$ with $N_b = 4$, 5, and 6 have maximal relative deviation 0.02% from those by $N_s = 5 \times 10^4$. For the attenuation constants, it requires larger N_s to converge the data. The largest relative deviation of the results obtained by $N_b = 4$, 5, and 6 is about 4% if $N_s \geq 2 \times 10^3$.

It is necessary to check if the results obtained by the program converge to correct values. In Fig. 2, the calculated attenuation constants using $N_b = 2$ through 6 for a microstrip are checked against the measured loss reported in [15]. The results obtained by $N_b = 3$ through 6 match the measurement very well all over the plotted frequency spectrum. The results by $N_b = 2$ are within the upper and lower limits of the measured data. Through the good match of the plots, it is safe to use $N_b = 4$ for accurate loss characterization of the microstrip lines. In Fig. 3, we compare the calculated effective dielectric constants $\epsilon_{\rm reff}$ for a pair of closely coupled microstrips with the measurement data in [12]. For both even and odd modes, the agreement between them is also quite good even for the $t = 0.25W_1 = 0.25S_2$ case.

Since the reliability of the MSDA technique has been established, $N_b = 4$ and $N_s = 5 \times 10^4$ are used for all the results shown herein. It takes about 4 min to calculate one data point on an HP735 machine.

B. Propagation and Attenuation Characteristics of Multimicrostrip Structures

A general N-line microstrip has N quasi-TEM eigenmodes. Each mode travels and attenuates independently along the waveguide with its own phase velocity and attenuation constant. The eigencurrent vectors for these modes are mutually independent and form a complete set. To observe wave propagation along the lines, one should express arbitrary excitations in terms of these eigenvectors [16].

The modal $\epsilon_{\rm reff}$ for two three-line microstrip structures with interline spacing 0.1 and 0.03 mm are plotted in Fig. 4(a) and (b), respectively. The results are shown for metallization thickness $t = 1, 5, 10$, and 15 μm. Modes 1, 2, and 3 are designated as those with eigencurrent vectors $[+\,+\,+]^{\mathbf{T}}$, $[+\delta-]^{\mathbf{T}}$, and $[+\,-\,+]^{\mathbf{T}}$, respectively, where δ is a number with relatively small magnitude. For all the modes, the $\epsilon_{\rm reff}$ values decrease when t value is increased as indicated by the arrows along with the plots. It can be seen that modes 1 and 3, respectively, have the least and the most variations of $\epsilon_{\rm reff}$ due to the change of the conductor thickness. Comparing the plots for each mode in Fig. 4(a) and (b), one can see that: a) the $\epsilon_{\rm reff}$ for mode 1 is relatively insensitive to the change of interline spacing; and b) the variations of the $\epsilon_{\rm reff}$ values for modes 2 and 3 due to the change of t values are increased as the interline spacing is decreased. These can be explained as follows. The field

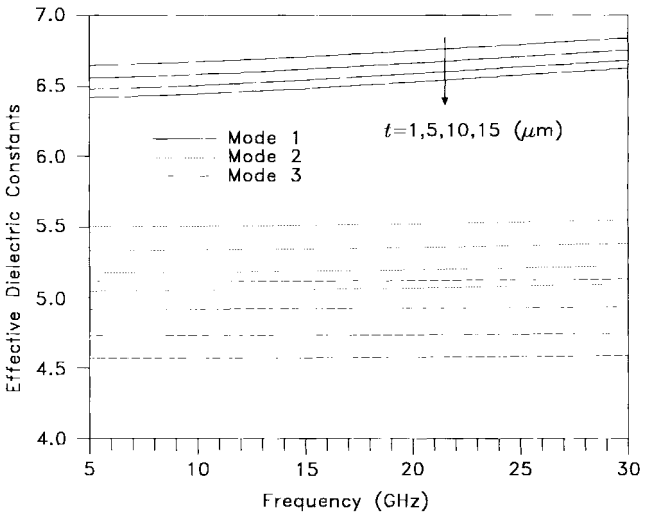

(a)

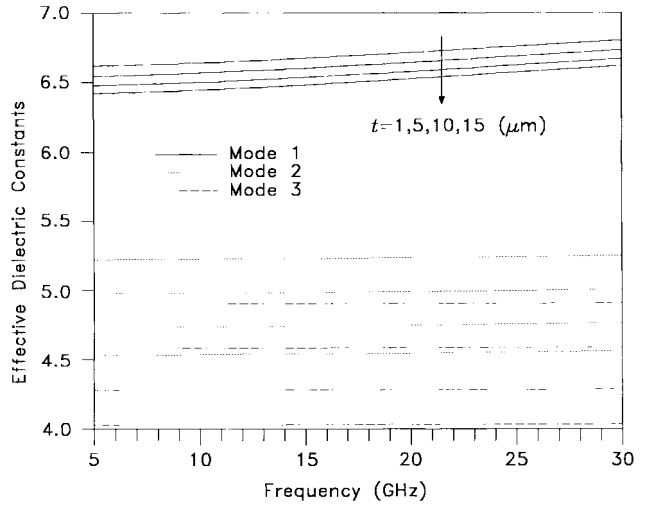

(b)

Fig. 4. Modal effective dielectric constants of three-line microstrip structures. $\epsilon_r = 8.875$, $W_1 = 0.08$ mm, $W_2 = 0.1$ mm, $W_3 = 0.06$ mm, $S_1 = S_4 = 1$ mm, $h_1 = 0.1$ mm, $h_2 = 2$ mm. (a) $S_2 = S_3 = 0.1$ mm. (b) $S_2 = S_3 = 0.03$ mm.

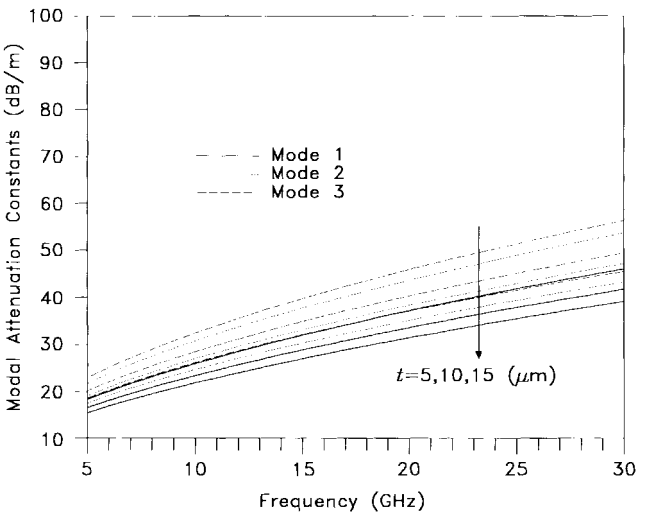

(a)

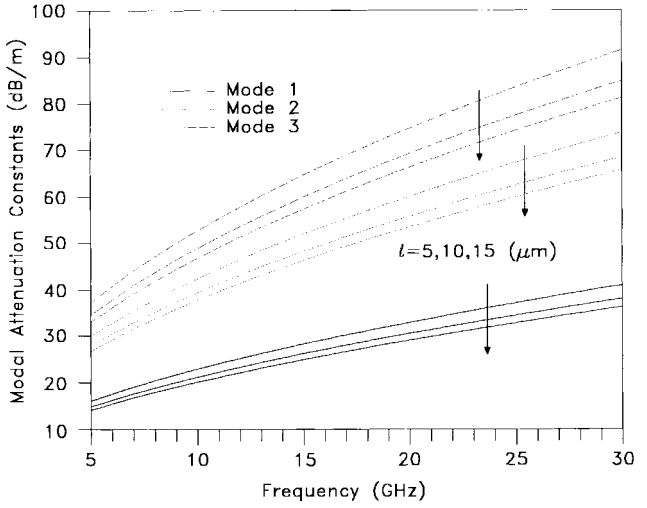

(b)

Fig. 5. Modal attenuation constants of three-line microstrip structures. Circuit parameters are in Fig. 4, $R_s = 4.1 \times 10^7$ S/m. (a) $S_2 = S_3 = 0.1$ mm. (b) $S_2 = S_3 = 0.03$ mm.

patterns for modes 1 and 3 are close to even modes while that for mode 2 is close to an odd one. Since for mode 3 the electric polarity of the central line is opposite to that of lines 1 and 3, when the three lines are placed closer or the metallization thickness is increased, the electromagnetic energy gathering around the interline air regions [cells 2 and 3 in Fig. 1(a) for $N = 3$] is increased. On the other hand, for mode 1, of which all lines are of the same polarity, most of fields concentrate in substrate, therefore the change of t or interline spacing has limited contributions to the variations of ϵ_{reff}.

Fig. 5(a) and (b) plot the attenuation constants for the three modes. Mode 1 has the smallest and mode 3 has the largest attenuation constants. For all the cases shown, the α values decrease as t is increased and increase as frequency is increased. It is interesting to note that, when the interline spacing is decreased from 0.1 mm [Fig. 5(a)] to 0.03 mm [Fig. 5(b)], the α values for mode 1 decrease slightly but those of modes 2 and 3 increase significantly.

Fig. 6(a) and (b) plot the effective dielectric constants for the four dominant modes of a four-line microstrip structure. The lines have identical width and are equally spaced. The four modes have eigencurrent vectors $[1\ R_1\ R_1\ 1]^{\text{T}}$, $[1\ R_2\ -R_2\ -1]^{\text{T}}$, $[1\ -R_3\ -R_3\ +1]^{\text{T}}$, and $[1-\ R_4\ +R_4\ -1]^{\text{T}}$, where R_1 through R_4 are positive constants. As shown in the plots, mode 1 and mode 4, respectively, present the most and the least dispersive propagation characteristics for any combination of t value and interline spacing.

The attenuation constants for the four-line structures are plotted in Fig. 7(a) and (b). In both plots, the α responses for different t values increase and spread out as frequency is increased. It implies that the dependence of the attenuation characteristics on the metallization thickness is increasingly important as frequency goes higher. Note that when the interline spacing is decreased from 0.254 mm [Fig. 7(a)] to 0.0762 mm [Fig. 7(b)], the difference among the α values for the four modes is significantly enlarged and, again, the α values for mode 1 decrease while those for the other three

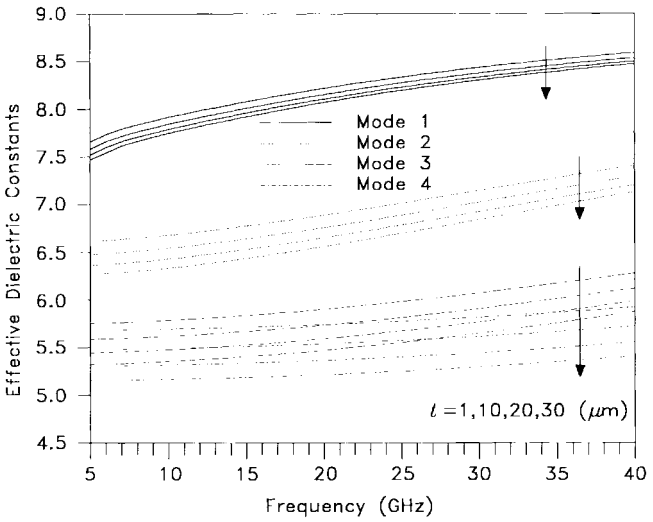

(a)

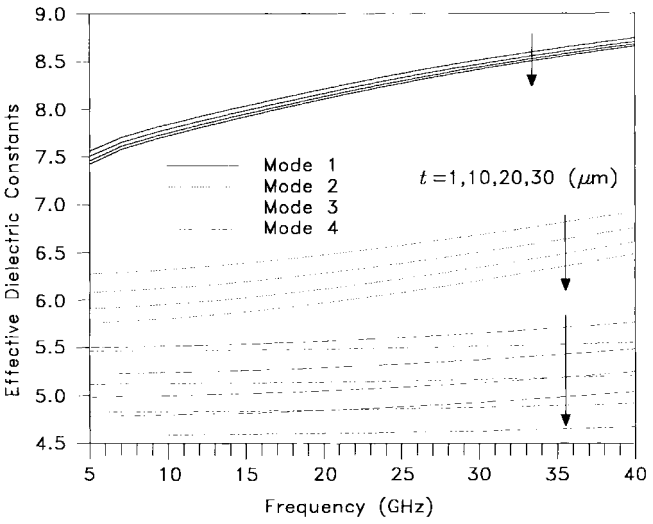

(b)

Fig. 6. Modal effective dielectric constants of four-line microstrip structures. $\epsilon_r = 9.9$, $W_1 = W_2 = W_3 = W_4 = h_1 = 0.254$ mm, $S_1 = S_5 = 2.54$ mm, $h_2 = 5$ mm. (a) $S_2 = S_3 = S_4 = 0.254$ mm. (b) $S_2 = S_3 = S_4 = 0.0762$ mm.

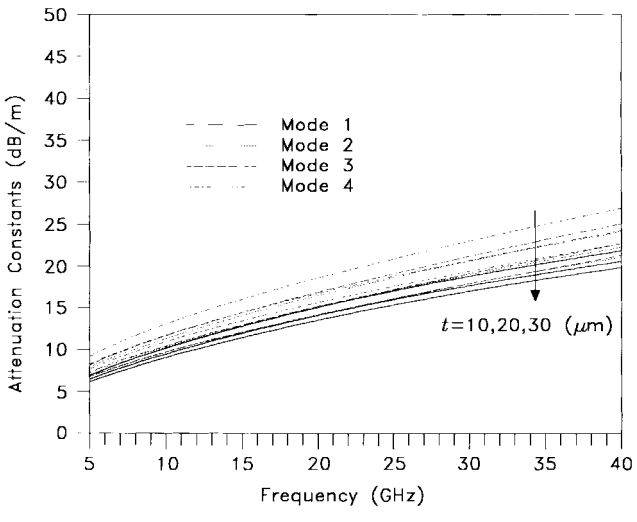

(a)

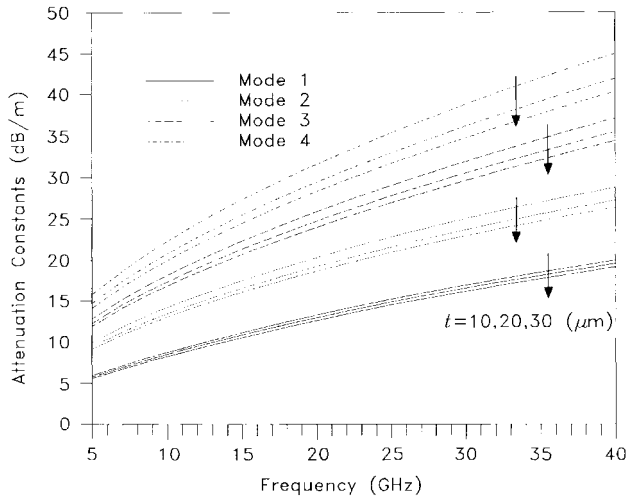

(b)

Fig. 7. Modal attenuation constants of four-line microstrip structures. Circuit parameters are in Fig. 6. $R_s = 4.1 \times 10^7$ S/m. (a) $S_2 = S_3 = S_4 = 0.254$ mm. (b) $S_2 = S_3 = S_4 = 0.0762$ mm.

modes increase. Mode 4 has the most dependence of α values on the interline spacing and metallization thickness.

IV. Conclusion

The MSDA has been successfully employed to analyze multiple coupled microstrip lines with arbitrary metallization thickness. The chosen set of basis functions has been proved to be effective in accurately calculating modal phase constants with merely hundreds of spectral terms. Based on the perturbation scheme, only four basis functions are sufficient for characterizing the metallic loss caused by the finite thickness microstrips up to millimeter-wave frequencies. It is found that the dependence of modal phase and attenuation constants of parallel coupled microstrips on the metallization thickness is significantly important, especially at higher microwave or millimeter-wave frequencies, and for the normal modes with relatively low effective dielectric constants.

References

[1] Z. Ma, E. Yamashita, and S. Xu, "Hybrid-mode analysis of planar transmission lines with arbitrary metallization cross sections," *IEEE Trans. Microwave Theory Tech.*, vol. 41, pp. 491–497, Mar. 1993.

[2] K. M. Rahman and C. Nguyen, "Full-wave analysis of coplanar strips considering the finite strip metallization thickness," *IEEE Trans. Microwave Theory Tech.*, vol. 42, pp. 2177–2179, Nov. 1994.

[3] W. Heinrich, "Full-wave analysis of conductor losses on MMIC transmission lines," *IEEE Trans. Microwave Theory Tech.*, vol. 38, pp. 1468–1472, Oct. 1990.

[4] C.-K. C. Tzuang, C.-D. Chen, and S.-T. Peng, "Full-wave analysis of lossy quasi-planar transmission lines incorporating the metal modes," *IEEE Trans. Microwave Theory Tech.*, vol. 38, pp. 1792–1799, Dec. 1990.

[5] C. Shih, R.-B. Wu, S.-K. Jeng, and C. H. Chen, "Frequency-dependent characteristics of open microstrip lines with finite strip thickness," *IEEE Trans. Microwave Theory Tech.*, vol. 37, pp. 793–795, Apr. 1989.

[6] M. S. Alam, K. Hirayama, Y. Hayashi, and M. Koshiba, "Analysis of shielded microstrip lines with arbitrary metallization cross section using a vector finite element method," *IEEE Trans. Microwave Theory Tech.*, vol. 42, pp. 2112–2116, Nov. 1994.

[7] F. J. Schmuckle and R. Pregla, "The method of lines for the analysis of planar waveguides with finite metallization thickness," *IEEE Trans. Microwave Theory Tech.*, vol. 39, pp. 107–111, Jan. 1991.

[8] T. Itoh and R. Mittra, "A technique for computing dispersion characteristics of shielded microstrip lines," *IEEE Trans. Microwave Theory Tech.,* vol. 22, pp. 896–898, Oct. 1974.
[9] T. Itoh, "Spectral domain immittance approach for dispersion characteristics of generalized printed transmission lines, *IEEE Trans. Microwave Theory Tech.,* vol. 28, pp. 733–736, July 1980.
[10] T. Kitazawa and T. Itoh, "Propagation characteristics of coplanar-type transmission lines with lossy media," *IEEE Trans. Microwave Theory Tech.,* vol. 39, pp. 1694–1700, Oct. 1991.
[11] T. Kitazawa, "Loss calculation of single and coupled strip lines by extended spectral domain approach," *IEEE Microwave Guided Wave Lett.,* vol. 3, pp. 211–213, July 1993.
[12] R. T. Kollipara and V. K. Tripathi, "Dispersion characteristics of moderately thick microstrip lines by the spectral domain method," *IEEE Microwave Guided Wave Lett.,* vol. 2, pp. 100–101, Mar. 1992.
[13] K. T. Ng and C. H. Chan, "Unified solution of various dielectric-loaded ridge waveguides with a mixed spectral-domain method," *IEEE Trans. Microwave Theory Tech.,* vol. 37, pp. 2080–2085, Dec. 1989.
[14] J.-T. Kuo and C.-K. C. Tzuang, "Complex modes in suspended coupled microstrip lines," *IEEE Trans. Microwave Theory Tech.,* vol. 38, pp. 1189–1197, Sep. 1990.
[15] M. E. Goldfarb and A. Platzker, "Losses in GaAs Microstrip," *IEEE Trans. Microwave Theory Tech.,* vol. 38, pp. 1957–1963, Dec. 1990.
[16] J.-T. Kuo and C.-K. C. Tzuang, "A termination scheme for high-speed pulse propagation on a system of tightly coupled coplanar strips," *IEEE Trans. Microwave Theory Tech.,* vol. 42, pp. 1008–1015, June 1994.

Jen-Tsai Kuo (S'88–M'92) received the B.S. degree in communication engineering from the national Chiao Tung University (NCTU), Taiwan, R.O.C., in 1981, the M.S. degree in electrical engineering from the National Taiwan University, Taiwan, R.O.C., in 1984, and the Ph.D. degree from the Institute of Electronics, NCTU, in 1992.

Since 1984, he has been with the Department of Communication Engineering at the NCTU as a Lecturer at both the Microwave and Communication Electronics Laboratories. From August 1995 to July 1996, he was a Visiting Scholar at the University of California, Los Angeles. His research interests include the analysis and design of high-frequency electronics and microwave circuits, high-speed interconnects and packages, field-theoretical studies of guided waves, and numerical techniques in electromagnetics.

Tatsuo Itoh (S'69–M'69–SM'74–F'82) received the Ph.D. degree in electrical engineering from the University of Illinois, Urbana, in 1969.

From 1966 to 1976, he was with the Electrical Engineering Department, University of Illinois. From 1976 to 1977, he was a Senior Research Engineer in the Radio Physics Laboratory, SRI International, Menlo Park, CA. From 1977 to 1978, he was an Associate Professor at the University of Kentucky, Lexington. In July 1978, he joined the faculty at The University of Texas at Austin, where he became a Professor of Electrical Engineering in 1981 and Director of the Electrical Engineering Research Laboratory in 1984. During the summer of 1979, he was a guest researcher at AEG-Telefunken, Ulm, Germany. In 1983, he was selected to hold the Hayden Head Centennial Professorship of Engineering at The University of Texas. In 1984, he was appointed Associate Chairman for Research and Planning of the Electrical and Computer Engineering Department at The University of Texas. In 1991, he joined the University of California, Los Angeles (UCLA), as Professor of Electrical Engineering and holder of the TRW Endowed Chair in Microwave and Millimeter Wave Electronics. He is currently Director of Joint Services Electronics Program (JSEP) and is also Director of Multidisciplinary University Research Initiative (MURI) program at UCLA. He was an Honorary Visiting Professor at Nanjin Institute of Technology, China, and at the Japan Defense Academy. In 1994, he was appointed Adjunct Research Officer for Communications Research Laboratory, Ministry of Post and Telecommunication, Japan. He currently holds a Visiting Professorship at University of Leeds, U.K. He has more than 200 journal publications, 350 refereed conference presentations in the area of microwaves, millimeter-waves, antennas, and numerical electromagnetics. He has supervised more than 30 Ph.D. students.

Dr. Itoh is a member of the Institute of Electronics and Communication Engineers of Japan and Commissions B and D of USNC/URSI. He served as the Editor of IEEE TRANSACTIONS ON MICROWAVE THEORY AND TECHNIQUES for 1983–1985. He serves on the Administrative Committee of IEEE Microwave Theory and Techniques Society. He was Vice-President of the Microwave Theory and Techniques Society in 1989 and President in 1990. He was the Editor-in-Chief of IEEE MICROWAVE AND GUIDED WAVE LETTERS from 1991 through 1994. He was elected as an Honorary Life member of MTT Society in 1994. He was the Chairman of USNC/URSI Commission D from 1988 to 1990, the Vice-Chairman of Commission D of the International URSI from 1991–1993, and is currently Chairman of the same Commission. He serves on advisory boards and committees of a number of organizations including the National Research Council and the Institute of Mobile and Satellite Communication, Germany.